Available online at www.sciencedirect.com

ScienceDirect

Journal of the European Ceramic Society 31 (2011) 869–876

www.elsevier.com/locate/jeurceramsoc

Chemical vapor deposition of carbon on particulate TiO_2 from CH_4 and subsequent carbothermal reduction for the synthesis of nanocrystalline TiC powders

S. Cetinkaya, S. Eroglu *

Istanbul University, Engineering Faculty, Dept. Metallurgical and Materials Eng., Avcilar, 34320 Istanbul, Turkey

Received 2 August 2010; received in revised form 9 November 2010; accepted 26 November 2010
Available online 17 December 2010

Abstract

The present study aims to investigate chemical vapor deposition of carbon from CH_4 on TiO_2 particles and to establish optimal conditions for the synthesis of nanocrystalline TiC powders. Mass measurements, XRD, HR-TEM and SEM were used to characterize the products at various stages of the reactions. Oxide particles gained mass rapidly at 1300 K under CH_4 atmosphere and were coated with thin pyrolytic carbon layers of 10–20 nm. XRD analysis showed that the coated powders consisted of C, TiO_2 and titanium sub-oxides. The powders containing $\sim 33 \pm 2$ wt% carbon were used for the carbothermal reduction of TiO_2 to TiC at 1600–1800 K under Ar flow. Lattice constant and mass loss of the samples increased to the levels of TiC with temperature and time. Nearly pure TiC powders with a mean particle size of ~125 nm were synthesized at 1750–1800 K within 30 min.

Keywords: Carbothermal reduction; Powder-solid state reaction; Carbides; X-ray methods; Microstructure-final

1. Introduction

Because titanium carbide (TiC) has high hardness, a high modulus of elasticity, a high melting point, good corrosion resistance, high thermal and electrical conductivities, it has been exploited in many areas ranging from cutting tools to nuclear materials. It is one of the most important starting constituents of sintered hard metals, steel bonded carbide components and plasma sprayed coatings for wear resistant applications.[1–3]

Demands for nanosized ceramic powders increase owing to improved properties (such as better densification, higher hardness, lower wear rate) in the products produced from them.[4] For example, it was reported[5] that the use of fine TiC particles prepared via carbothermal reduction of TiO_2 with carbon coating resulted in higher density compared to commercial TiC in the Ni–TiC compacts.

Various methods have been developed for the synthesis of fine TiC powders including carbothermal reduction,[6] thermal plasma,[7] vapor phase reaction or chemical vapor deposition[8] and reactive ball milling.[9] It appears that none of them is utilized for commercial production mainly due to high costs, corrosive precursors, process complexity and poor product purity. For example, chemical vapor deposition technique employs corrosive, expensive titanium compounds (e.g. $TiCl_4$) as a titanium source along with hydrocarbons and hydrogen.

Carbothermal reduction of TiO_2 powders mixed with solid carbon black is used industrially due to its ease of operation and low cost.[1,10,11] This method, however, requires high temperatures (>2000 K) and long reaction times (>10 h) owing to sluggish reaction rates between separate TiO_2 and C particles resulting in coarse TiC particles of low purity. Particle size of the powders can be reduced to >150 nm by a cumbersome and time consuming milling process. Furthermore, products are contaminated by the solid carbon with impurities like Ca, Si, Fe, S, and P and by milling media. In spite of its disadvantages, conventional carbothermal reduction appears to be the most promising method for industrial production of fine TiC powders. The problems

---

* Corresponding author. Tel.: +90 212 473 7065; fax: +90 212 473 7180.
E-mail addresses: seref@istanbul.edu.tr, serafettine63@gmail.com (S. Eroglu).

0955-2219/$ – see front matter © 2010 Elsevier Ltd. All rights reserved.
doi:10.1016/j.jeurceramsoc.2010.11.027

associated with the technique may be circumvented by using fine grained TiO_2 precursor and by providing closer contact area between the precursors. So that enhanced carbothermal reaction can take place at lower temperatures in shorter times owing to short-diffusion paths and increased C uptake. Intimate contact between C and TiO_2 may be best achieved by coating oxide particles with carbon from gas-phase, which also improves product purity and minimizes particle coarsening. It was reported[6] that titania nanoparticles were coated with carbon by thermal cracking of C_3H_6 (propylene) at elevated pressure and at 873 K. Up to 18 cycles, each lasting ~20 min, were necessary to achieve 32–34 wt% of carbon required for the subsequent conversion of TiO_2 to TiC. Multicycle C coating process and carbothermal reduction in a separate vessel seem to limit the industrial use of the method. It is therefore apparent that a fast and economical process for producing fine TiC powder is presently needed.

Recently, titanium oxide particles coated with carbon by heat treatment of the powder mixture of rutile-type TiO_2 with polyvinyl alcohol in inert atmosphere have received considerable attention for the use as a photocatalyst in the area of environment conservation and remediation.[12] Hence, it is worthy of studying carbon coating processes using different techniques and precursors for possible alternative routes to carbon encapsulated TiO_2 particle synthesis.

Until now, there is no published report on chemical vapor deposition of carbon from CH_4 on the particulate TiO_2. In the present study, we used CH_4 gas as a carbon source because it is relatively cheap and abundant. The present study also demonstrated that TiC powders with finer particle size could be synthesized in a shorter time at 1750–1800 K using the composite precursor obtained from CH_4 compared to the earlier works.[5,6] Furthermore, the present study shows that both carbon coating and TiC synthesis steps can be carried out in the same reactor by allowing CH_4 flow during heating-up and switching to Ar at higher temperatures. Hence, the process presented here has inherent advantages, including a simple flexible production procedure, low cost carbon source and short synthesis time and can be easily scaled up. Consequently, the present work was undertaken in order to establish optimal conditions for the formations of nanocrystalline carbon shell–titanium oxide composite particles and TiC powders. Furthermore, detailed equilibrium thermodynamic analysis in the Ti–O–C–Ar system using Gibbs' free energy minimization method was also carried out in order to get a deeper insight into the thermochemistry of the carbothermal reduction process.

2. Thermodynamic analysis of carbothermal reduction of TiO_2 by carbon

Equilibrium thermodynamic analysis has been carried out by the method of minimization of the Gibbs' free energy of a system,[13] obeying mass constraint. For a system of known input composition, it computes equilibrium gas phase and condensed phase compositions at a given pressure and temperature. The calculation requires specifying all possible species and condensed phases known to exist in the temperature range of interest. For the carbothermal reduction of TiO_2 by carbon in Ar atmosphere, the species considered as the constituents of the gas phase included Ar, CO, CO_2, Ti, TiO, TiO_2, O_2 and O. Condensed equilibrium phases were assumed to be pure C, TiO_2, titanium sub-oxides (Ti_4O_7, Ti_3O_5, Ti_2O_3, and TiO), Ti and TiC. Input thermodynamic data in the form of Gibbs' free energy of the formation of the constituents considered in the present study were obtained from the thermochemical tables.[14,15]

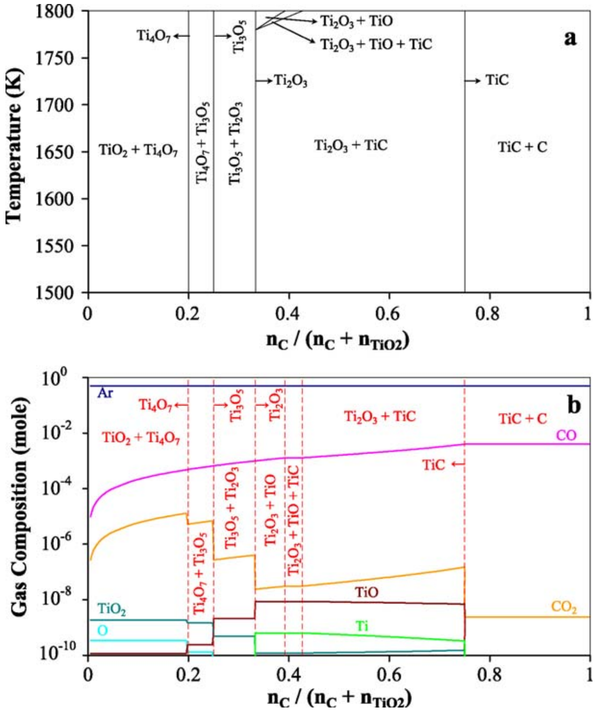

Fig. 1. (a) The equilibrium solid stability diagrams showing phase fields as a function of temperature and input carbon mole fraction. (b) Variation of equilibrium gas composition with input carbon mole fraction at 1800 K. Ar content is 0.5 mole.

Thermodynamic calculations of complex equilibria in the system of TiO_2–C–Ar were performed using a modified version of Eriksson's computer program SOLGAS-MIX[16] for input carbon mole fraction in the range 0–1 at atmospheric pressure and at temperatures of 1500–1800 K. Fig. 1 depicts the diagrams constructed from the calculated results. An equilibrium stability diagram for the condensed phases is displayed in Fig. 1a. The boundary lines in the diagram divide different phase fields in which the indicated phases are expected to form. The information obtained from the figure can be summarized as follows. The equilibrium line compounds of pure Ti_4O_7, Ti_3O_5, Ti_2O_3 and TiC are expected at carbon mole fractions of 0.2, 0.25, 0.33 and 0.75, respectively. Formation of TiC is predicted along with Ti_2O_3 phase at mole fractions between 0.33 and 0.75. Above 0.75, free C coexists with TiC. Ti_2O_3 + TiO and Ti_2O_3 + TiO + TiC phase fields are also seen at temperatures near 1800 K and at mole fractions ~0.4.

In order to gain more insight into thermochemistry of the process, gas phase composition at 1800 K was studied as input carbon mole fraction varied. Hence, possible chemical reaction pathways to the formation of TiC could be suggested using the contents of products and the input reactants. Fig. 1b shows the composition of the gas phase. Vertical lines shown in the figure separate the condensed phase fields corresponding to those in Fig. 1a. As seen from the figure, the gaseous species expected to form are CO, CO_2, TiO_2, TiO, Ti and O. Among these species, CO has the highest concentration at all input mole fractions and its content increases with the input mole fraction up to 0.75 above which it becomes constant. The concentration of CO_2 is predicted to be much less than that of CO. The amounts of the other species are found to be very small.

Based on the calculations, the titanium sub-oxide phases (for example, Ti_nO_{2n-1} phases with $1 \leq n \leq 4$) and major gaseous species are expected to form at low C mole fractions by the following reactions:

$$n\mathrm{TiO_2} + \mathrm{C} \rightarrow \mathrm{Ti}_n\mathrm{O}_{2n-1} + \mathrm{CO} \quad (1)$$

$$n\mathrm{TiO_2} + 1/2\mathrm{C} \rightarrow \mathrm{Ti}_n\mathrm{O}_{2n-1} + 1/2\mathrm{CO_2} \quad (2)$$

$$\mathrm{CO_2} + \mathrm{C} \rightarrow 2\mathrm{CO} \quad (3)$$

The equilibrium analysis suggests that TiC may form from lower titanium oxides TiO or Ti_2O_3 depending on temperature possibly through the intermediate reactions of:

$$\mathrm{Ti}_n\mathrm{O}_{2n-1} + (3n-1)\mathrm{C} \rightarrow n\mathrm{TiC} + (2n-1)\mathrm{CO} \quad (4)$$

$$\mathrm{Ti}_n\mathrm{O}_{2n-1} + (4n-1)/2\mathrm{C} \rightarrow n\mathrm{TiC} + (2n-1)/2\mathrm{CO_2} \quad (5)$$

where n is 1 or 2. This result is consistent with the experimental literature.[6,10]

TiC is predicted to form by the following net reaction which may be viewed as the total of reactions (1) and (4) or (2), (3) and (5):

$$\mathrm{TiO_2} + 3\mathrm{C} \rightarrow \mathrm{TiC} + 2\mathrm{CO} \quad (6)$$

Eq. (6) is the well known overall reaction for the carbothermal reduction of TiO_2 to TiC by solid carbon.

3. Experimental procedures

The experimental setup used for the present study essentially consists of a hot-wall tubular alumina furnace (20 mm in diameter) with SiC heating elements and gas flow meters. The details of the reactor are given elsewhere.[17] The chemicals used were TiO_2 powder (99.7%), high purity argon (99.999%) and methane (99.5%). Particle size of the TiO_2 powder was reported to be <25 nm by the producer (Sigma–Aldrich). The alumina boat with gas entrance side cut to allow smooth gas flow was loaded with the reactant powders. Prior to the experiments, the powders were held at 373 K in an oven for moisture removal. Mass measurements before and after experiments were carried out by a calibrated electronic balance (Sartorius BP110S) with a sensitivity of $\pm 10^{-4}$ g in order to determine the extent of the reactions. Change in mass was calculated using the equation of $(m - m_0)/m_0 \times 100$ where m is the mass at temperature T or time t and m_0 is the starting mass of the sample.

The experiments consisted of two successive steps: (i) chemical vapor deposition of carbon on the oxide particles from pure CH_4 and (ii) subsequent carbothermal reduction under Ar atmosphere. In the first step, the oxide powders (∼80 mg) were heated at a rate of 25 K/min in flowing CH_4 (40 cm^3/min) and were isothermally held at 1300 K to deposit carbon on the particulate oxide for the subsequent carbothermal reaction. Carbon content of the coated samples was determined by burning it off in air at 900 K for ∼10 min. In the second step, the carbon coated oxide powders (∼200 mg) were heated up to the temperatures of 1600–1800 K and kept at these temperatures for different periods of time under Ar flow (250 cm^3/min). The reaction products were allowed to cool in the Ar atmosphere.

Morphology of the carbon coated powders was examined by a High Resolution Transmission Electron Microscope (JEOL 2100 LaB_6 HR-TEM). For this examination, the powder was mixed with ethanol and the mixture was then dropped on the TEM grid. A Scanning Electron Microscope (JEOL 6335 FEG-SEM) equipped with Field Emission Gun was employed to reveal morphologies of carbothermal reaction products. Mean particle sizes were determined from the areas of at least 80 particles using an image analysis program (UTHSCSA Image Tool) and FEG-SEM images. Equivalent circular diameters of the measured areas were calculated to describe mean particle sizes.

Phase analyses were performed using a parafocusing X-ray diffractometer (RIGAKU D/Max-2200 XRD) equipped with a Cu radiation tube and a monochrometer. The crystallite size was calculated from the X-ray diffraction peak profiles using the Scherrer formula:

$$t = \frac{\lambda}{\beta \cos\theta} \quad (7)$$

where λ is the wavelength of Cu K_α radiation (0.15418 nm), θ is the diffraction angle, t is the crystallite size and β is the full breadth of the diffraction peak from the (2 0 0) crystallographic plane at half-maximum intensity which was corrected for instrumental broadening (∼0.2°). Precise lattice constants of the products were measured using high angle diffraction peaks with $2\theta > 100°$ in order to determine the extent of the carbothermal reduction. For this analysis, the diffraction angles of the (3 3 1), (4 2 0), (4 2 2) and (5 1 1,3 3 3) crystallographic planes were determined by fitting a parabola to the top portion of the peak and taking the axis of the parabola as the peak center.[18] Precise lattice constant was then calculated at $2\theta = 180°$ using $\sin^2\theta$ extrapolation function and the lattice constants of the peaks measured.

4. Results and discussion

4.1. Chemical vapor deposition of carbon on titanium oxide particles

Fig. 2 shows the change in mass of the powders heated-up to 1300 K under CH_4 atmosphere. As seen from the figure, mass initially decreases as temperature is raised to 900 K at which a mass loss of ∼3.45 wt% is attained. The loss is attributed to the partial removal of oxygen from TiO_2 in CH_4 atmosphere as will be shown by the XRD analysis later. At temperatures between 900 and 1200 K, the samples slowly gain mass with increasing temperature due to carbon deposition. The color of the products

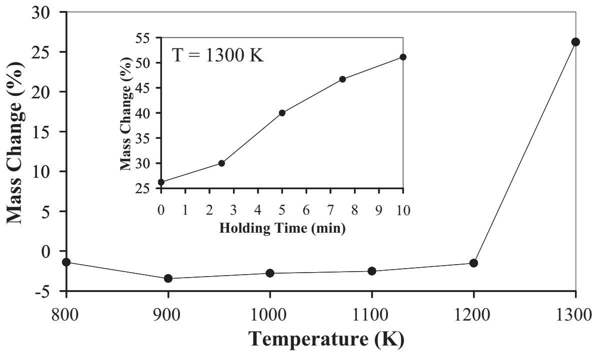

Fig. 2. Change in mass of the starting TiO_2 powder after heating up to the target temperatures of 800–1300 K under CH_4 flow. The inset shows the effect of isothermal holding time on mass change at 1300 K.

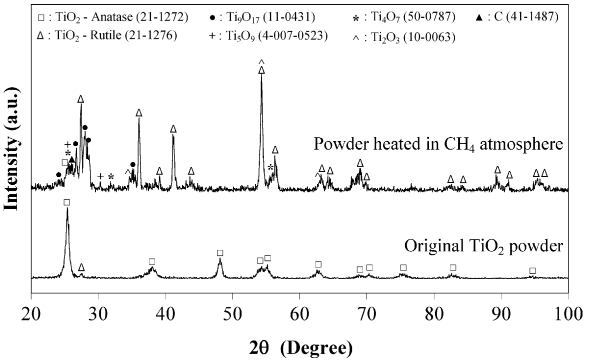

Fig. 3. XRD patterns of the starting TiO_2 powder and the product obtained under methane atmosphere at 1300 K for isothermal time of 5 min. PDF numbers of the matched materials are also shown in the parentheses.

was observed to change progressively from white at 900 K to dark gray at 1200 K. At 1300 K, a rapid rise in mass to 26 wt% is seen owing to more C uptake indicating CH_4 decomposes appreciably at the temperature. The inset in Fig. 2 shows further increase in mass with rising isothermal holding time at 1300 K (max. 51 wt% at 10 min).

The selection of the carbon coated powders for the subsequent carbothermal reaction is explained as follows. Owing to the oxygen loss from TiO_2, slightly less carbon is needed compared to the theoretical one (mass change of 45 wt%) required in accordance with Eq. (6). The powders with a mass change of 40 wt% (slightly less than 45 wt%) prepared at 1300 K for isothermal holding time of 5 min seemed to be a good choice for the complete reduction of TiO_2 to TiC without too much free carbon in the final product.

It should be mentioned that Fig. 2 does not yield directly the carbon content of the products or oxygen loss from TiO_2 because carbon mass gain is masked by oxygen loss at temperatures >900 K. Hence, carbon was burned off in air to determine its content in the coated product by a simple calculation using the mass of the carbon coated powder and the residual mass. Carbon concentrations in the products at 1300 K were found to be ~26 wt% and ~33 wt% for isothermal holding periods of 0 and 5 min, respectively. It was also noted that the mass remained after carbon burned at 900 K within 10 min was less than that of the initial TiO_2, indicating that sub-oxides were not converted to TiO_2. It was reported[19] that oxidation of the titanium sub-oxides to TiO_2 takes hours in an oxygen stream at 1273 K. Hence, approximated oxygen loss during the coating process was also calculated using the residual mass and the initial mass of TiO_2. Oxygen loss was estimated to increase from ~3.45 wt% at 900 K (no carbon deposition observed at this temperature) to ~6.65 wt% of the initial TiO_2 mass at 1300 K. Considering the oxygen deficiency in the titanium oxide, Eq. (6) may be re-expressed as

$$TiO_{2-x} + (3-x)C \rightarrow TiC + (2-x)CO \qquad (8)$$

where x is estimated to be 0.332 at 1300 K. The amount of C required for the formation of TiC in accordance with this reaction was then determined to be 30 wt%. The powder coated with carbon at 1300 K for 5 min attained a mean carbon content of $\sim 33 \pm 2$ wt%. Hence, this product with a slightly excessive carbon was used for the subsequent carbothermal reaction to ensure that the formation of TiC is complete.

XRD patterns of the starting TiO_2 powder and the carbon coated product obtained under CH_4 atmosphere at 1300 K for isothermal time of 5 min are shown in Fig. 3. Original TiO_2 powder consists of major anatase and minor rutile phases whose peak intensities and diffraction angles are found to be in agreement with published values.[20] The pattern of the coated product exhibits peaks from a mixture of rutile, anatase, carbon and titanium sub-oxide phases. The presence of the sub-oxide phases confirms the mass loss observed during the coating. After heating in CH_4 atmosphere, anatase mostly transformed to rutile as expected. The identification of the sub oxide peaks in the pattern was problematic due to peak overlapping. Nevertheless, they were ascribed to Ti_9O_{17}, Ti_5O_9, Ti_4O_7 and Ti_2O_3 phases. Thermodynamic calculations (details not presented here) in the TiO_2–CH_4 system at 1300 K indicated that TiO_2, titanium suboxides and carbon are the expected phases, while TiC forms in negligible amount. Hence, it is reasonable to propose that oxygen loss from TiO_2 is due to the partial reduction of TiO_2 by CH_4 which may take place through the following reaction:

$$nTiO_2 + CH_4 \rightarrow Ti_nO_{2n-1} + CO + 2H_2 \qquad (9)$$

Typical HR-TEM morphology of the products obtained at 1300 K for 5 min is shown in Fig. 4a–c at various magnifications. As clearly seen from the images, the oxide particles were homogeneously coated with carbon layers with a thickness of 10–20 nm. The high resolution image of the product reveals that pyrolytic carbon coating is composed of (0 0 2) basal planes with interplanar spacing of ~0.34 nm, in reasonable agreement with the well known value of 0.336 nm of highly crystalline graphite. The particle size of the oxide was measured to be 85 ± 35 nm based on the measurements from the multiple images, indicating that particle coarsening took place during heating-up. Mean crystallite size of rutile phase calculated by Eq. (7) was found to be 75 nm, suggesting that particles are mostly monocrystalline in nature.

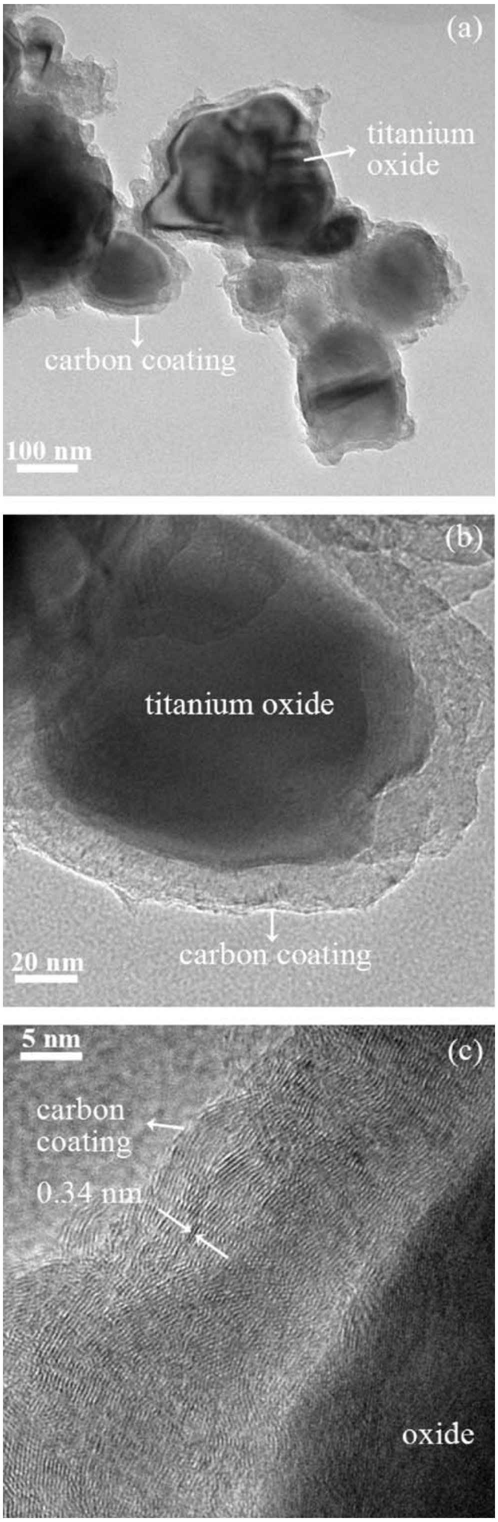

Fig. 4. HR-TEM images of the oxide powder coated with pyrolytic carbon at 1300 K for isothermal holding time of 5 min in CH_4 atmosphere.

4.2. Synthesis of TiC by carbothermal reduction

Fig. 5 shows change in sample mass as a function carbothermal reaction temperature and time. As seen from the figure, the mass loss increases with temperature and isothermal holding time indicating that extent of the carbothermal reaction increases. The mass loss data at 0 min illustrate that carbothermal reduction takes place significantly during heating to the target temperatures. For example, it increases to 15.2% at 1600 K and to 42.3% at 1800 K. As also seen from the figure, mass loss slightly increases with time at 1750 and 1800 K. After 30 min of reaction time, it was measured to be ~42.1% at 1750 K and 42.4% at 1800 K, close to the theoretical value (41.77 wt%) estimated in accordance with Eq. (8) (excessive carbon included for the calculation). This result suggests that the carbothermal reaction is complete.

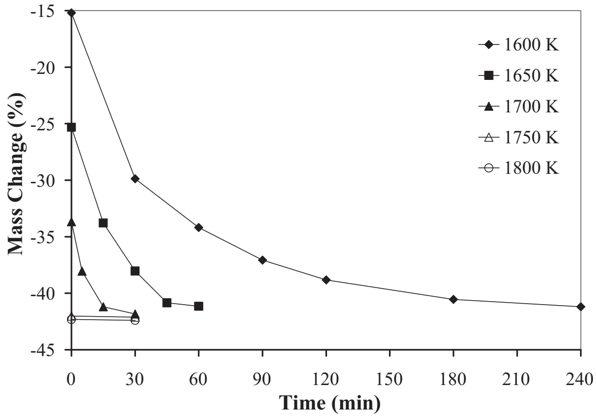

Fig. 5. Influence of carbothermal reaction temperature and isothermal holding time on the mass change (mass loss) in the carbon coated oxide powders.

Fig. 6 displays the XRD patterns of the powders for initial (0 min) and final holding times. At lower temperatures of 1600–1650 K for 0 min, it appears from the patterns that the

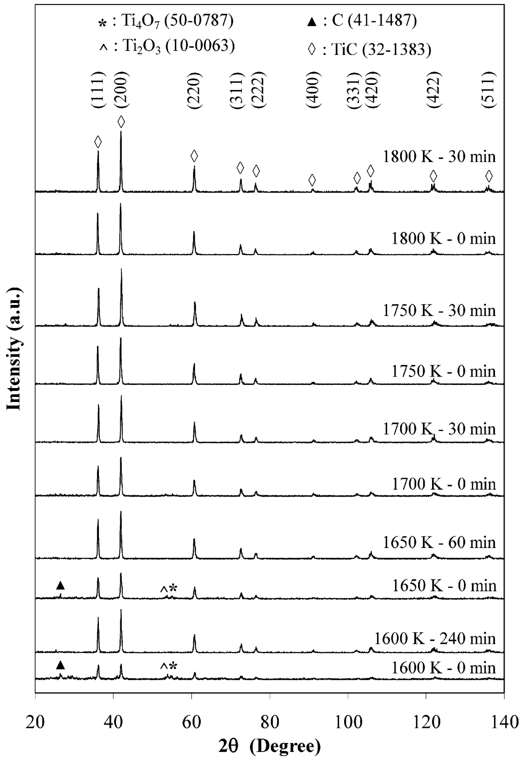

Fig. 6. XRD patterns of the products obtained by carbothermal reaction at temperatures between 1600 and 1800 K for zero and final holding times.

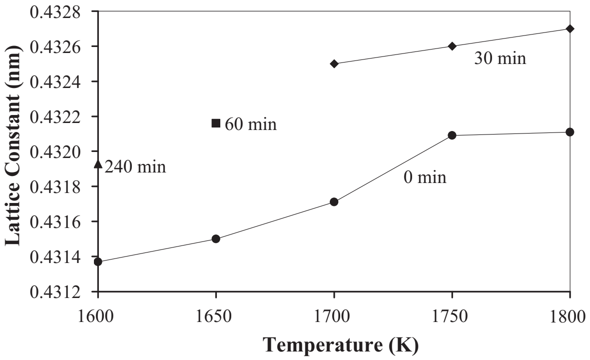

Fig. 7. Variation of lattice constant of the samples with carbothermal reaction temperature and time.

reaction products contain a major carbide phase, minor phases of C and titanium sub-oxides (Ti_4O_7, Ti_2O_3). With increasing time and temperature, the minor phases disappear while the carbide content increases as comparative analysis of peak intensities indicate. At higher temperatures of 1750–1800 K, the XRD patterns consist of diffraction peaks only from the carbide containing phase. It was observed that the diffraction angles shift slightly towards lower angles with increasing temperature and time, meaning that lattice constant increases. It is well known that TiC forms a solid solution with TiO and the lattice constant of the solution increases with decreasing oxygen content.[1,6,21] Hence, the shift to lower angles is ascribed to increased purification of the samples. The precise lattice constants of the products were compared with the published values for pure TiC (0.4328–0.4327 nm).[20,22] The calculated lattice constants from the XRD patterns are shown in Fig. 7 as a function

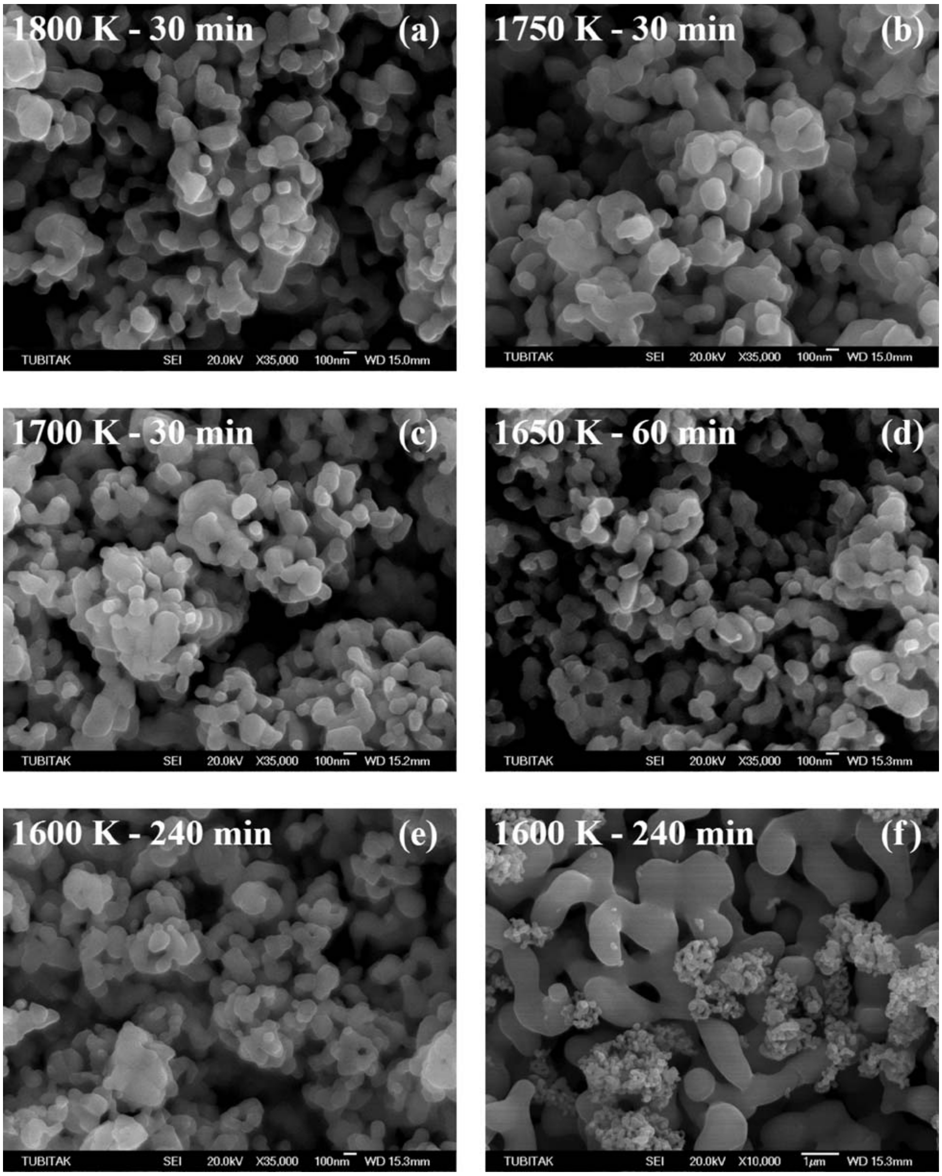

Fig. 8. FEG-SEM images of the products after carbothermal reaction. Reaction temperature and isothermal holding time are shown on the images (a)–(f). The powder prepared at 1600 K for 240 min exhibits fine (e) and coarse particles (f).

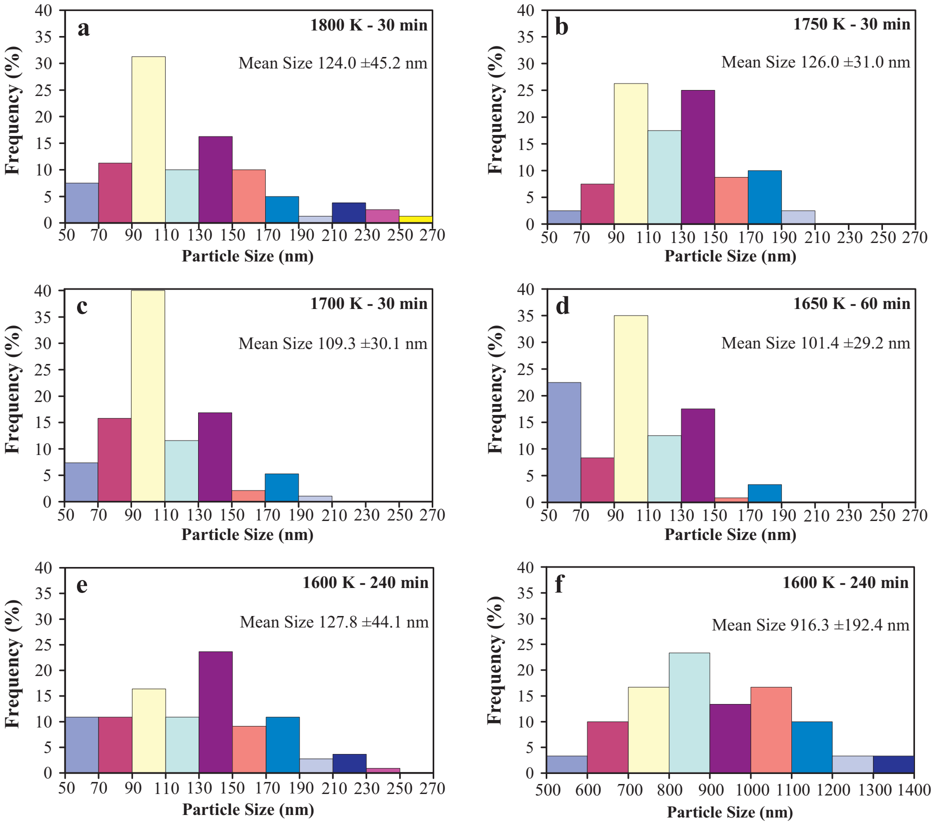

Fig. 9. Particle size distribution in the carbothermal reaction products. Reaction temperature, isothermal holding time and mean size are shown on the histograms (a)–(f). The powder prepared at 1600 K for 240 min exhibits a bimodal particle size distribution (e–f).

of temperature and time. As can be seen from the figure, lattice constant increases with temperature and time. For example, it increases from ~0.4314 nm at 1600 K to ~0.4321 nm at 1800 K for isothermal holding period of zero min. A maximum value of 0.4327 nm was reached at 1800 K within 30 min, indicating that almost pure TiC formed.

The mean crystallite size of the products was estimated from the XRD peak profiles using Eq. (7). It increased from 68 to 95 nm when carbothermal reaction temperature was raised from 1600 to 1800 K for zero holding time. The products obtained at the final carbothermal reduction times had crystallite sizes of 117 nm at 1600 K for 240 min and 84 nm at 1650 K for 60 min. At temperatures between 1700 and 1800 K for the 30 min, it increased from 100 to 128 nm with temperature. These results indicate that grain coarsening took place during carbothermal reduction.

The powders produced were observed to flow freely. Fig. 8 shows the particle morphologies after the carbothermal reduction. They are generally composed of homogeneously distributed fine, almost round particles with loose agglomeration. It is interesting to note that at 1600 K for 240 min reaction time, the morphology (Fig. 8e–f) is different from the others; it consists of fine particles as well as coarse particles. Coarse particles were formed as a result of sintering owing to prolonged holding time.

Fig. 9 shows particle size distribution and mean particle size of the powders displayed in Fig. 8. As can be seen from Fig. 9a–c, mean particle size increases with temperature from 109 ± 30 nm at 1700 K to 124 ± 45 nm at 1800 K for 30 min reaction time. At 1650 K, it was measured to be 101 ± 29 nm for 60 min holding time (Fig. 9d). At 1600 K for 240 min, the product exhibits a bimodal particle size distribution and mean particle size for each mode is measured to be 128 ± 44 and 916 ± 192 nm (Fig. 9e–f). It should be noted that the crystallite size of the final products generally seems to agree with the particle size measurements obtained from the SEM images indicating that the particles are mostly monocrystalline in nature. It should be emphasized that TiC powders with a finer mean particle size were synthesized in a shorter time at 1750–1800 K using the composite precursor obtained from CH_4 compared to those (1773 K – 2 h and 1823 K – 4 h) reported in the earlier works.[5,6] This result can be attributed to the partial reduction of TiO_2 during the coating process and to more homogeneous carbon coating, thus reducing synthesis time for subsequent carbothermal conversion to TiC. Other advantage of the approach presented here is that both carbon coated oxide particle and TiC powder synthesis steps can be carried out in the same reactor; CH_4 flow during heating-up results in oxide particles encapsulated with carbon and after coating process switching to Ar at higher temperatures yields TiC powders.

5. Conclusions

Chemical vapor deposition from pure CH_4 at 1300 K for 5 min resulted in significant amount of carbon deposit

(∼33 wt%) on the oxide particles. Oxygen loss occurred owing to partial reduction of TiO_2 by CH_4 during the coating process. HR-TEM revealed that titanium oxide particles were homogeneously coated with pyrolytic carbon layer of 10–20 nm. Equilibrium thermodynamic analysis in the TiO_2–C–Ar system indicated that TiC forms via TiO or Ti_2O_3 intermediate phases at 1500–1800 K. Precise lattice constant and mass loss measurements revealed that the extent of carbothermal reaction in the carbon coated oxide powders increased to the level of TiC with rising temperature and time. Nearly pure TiC powders with a mean particle size of ∼125 nm were synthesized at 1750–1800 K for 30 min. It was demonstrated that nanocrystalline carbon shell–titanium oxide core composite particles and pure TiC powders could be produced in the same reactor via chemical vapor deposition of carbon from methane and subsequent carbothermal reduction.

Acknowledgements

This work was supported by Scientific Research Projects Coordination Unit of Istanbul University (Project Number 1453). It was partially based on a Ph.D. thesis being pursued by S. Cetinkaya.

References

1. Schwarzkopf P, Kieffer R. *Refractory hard metals*. New York: The Macmillan Company; 1953.
2. Davis JR, editor. *ASM specialty handbook: tool materials*. Materials Park, OH: ASM International; 1995.
3. Matejka D, Benko B. *Plasma spraying of metallic and ceramic materials*. New York: John Wiley & Sons; 1989.
4. Kear BH, McCandlish LE. Nanostructured W-base materials synthesis processing and properties. *J Adv Mater* 1993;**25**:11–9.
5. Swift GA, Koc R. Formation studies of TiC from carbon coated TiO_2. *J Mater Sci* 1999;**34**:3083–93.
6. Koc R, Folmer JS. Carbothermal synthesis of titanium carbide using ultrafine titania powders. *J Mater Sci* 1997;**32**:3101–11.
7. Tong L, Reddy RG. Synthesis of titanium carbide nano-powders by thermal plasma. *Scripta Mater* 2005;**52**:1253–8.
8. Okabe Y, Hojo J, Kato A. Formation of fine titanium carbide powders by a vapor phase reaction. *Yogyo-Kyokai-Shi* 1978;**88**:518–26 [in Japanese].
9. Lohse BH, Calka A, Wexler D. Synthesis of TiC by controlled ball milling of titanium and carbon. *J Mater Sci* 2007;**42**:669–75.
10. Berger LM. Titanium carbide synthesis from titanium dioxide and carbon black. *J Hard Mater* 1992;**3**:3–15.
11. Maitre A, Tetard D, Lefort P. Role of some technological parameters during carburizing titanium dioxide. *J Eur Ceram Soc* 2000;**20**:15–22.
12. Kim TW, Lee MJ, Moon H. Preparation and characterization of carbon-coated TiO_2 for photocatalytic degradation of organic compounds. *J Future Fusion Tech* 2009;**1**:13–8.
13. Eriksson G. Thermodynamic studies of high temperature equilibrium. *Chem Scripta* 1975;**8**:100–3.
14. Chase MW, Davies CA, Downey JR, Frurip DJ, McDonald RA, Syverud AN. *JANAF thermochemical tables*. 3rd ed. *J Phys Chem Ref Data* 1985;**14**(Suppl. 1).
15. Barin I. *Thermochemical data of pure substances*. Weinheim: VCH Verlagsgesellschaft; 1993.
16. Besmann TM. *SOLGASMIX-PV, a computer program to calculate equilibrium relationships in complex chemical systems*. Oak Ridge National Laboratory: Report No. ORNL/TM-5775; 1977.
17. Cetinkaya S, Eroglu S. Thermodynamic analysis and synthesis of porous Mo_2C sponge by vapor-phase condensation and in situ carburization of MoO_3. *J Alloys Compd* 2010;**489**:36–41.
18. Cullity BD. *Elements of X-ray diffraction*. 2nd ed. Reading, MA: Addison-Wesley Publishing Company; 1978.
19. Andersson S, Collen B, Kuylenstierna U, Magneli A. Phase analysis in the titanium–oxygen system. *Acta Chem Scand* 1957;**11**:1641–52.
20. *Joint Committee on Powder Diffraction Standards*. Swartmore, PA: International Center for Diffraction Data; 2008.
21. Woo YC, Kang HJ, Kim DJ. Formation of TiC particle during carbothermal reduction of TiO_2. *J Eur Ceram Soc* 2007;**27**:719–22.
22. Eroglu S, Gallois B. Growth and structure of TiC coatings chemically vapor deposited on graphite substrates. *J Mater Sci* 1995;**30**:1754–9.